Metrol. Meas. Syst., Vol. 32 (2025) No. 4, pp. 1–14
DOI: 10.24425/mms.2025.155808

PAN POLSKA AKADEMIA NAUK

METROLOGY AND MEASUREMENT SYSTEMS
Index 330930, ISSN 0860-8229
www.metrology.wat.edu.pl

M&MS

MEASUREMENT OF BULK DENSITY USING THE ARCHIMEDES METHOD WITH AN INDUCTIVE SPRING BALANCE

Janusz Nurkowski, Maciej Tram, Barbara Dutka

Strata Mechanics Research Institute of the Polish Academy of Sciences, ul. Reymonta 27, 30-059 Kraków, Poland
(✉ *dutka@imgpan.pl*)

Abstract

The article presents a new version of the hydrostatic method for determining bulk density. A spring balance was designed and constructed for measuring the bulk density of porous samples using the liquid displacement method (Archimedes' principle). In the innovative spring balance, a weight-to-frequency converter based on an LC oscillator was used, in which the sensor consists of springs that simultaneously serve as the source of inductance in the oscillator's resonant circuit. Changes in inductance caused by the variation in the spring length under the load of the weighed object result in a change in oscillation frequency. The spring balance design is characterized by great simplicity, and the converter has a high sensitivity at the level of 10^{-5}. In this work, the bulk density of reference samples, both porous and non-porous, was investigated. The results of bulk density measurements for aluminium block and porous sandstone were compared with values obtained from professional pycnometers, namely, the helium AccuPyc 1340 and the quasi-liquid (powder) GeoPyc 1360 (Micromeritics Instrument Corporation, United States). The results confirm the full suitability of the spring balance for the intended purpose.

Keywords: spring balance, bulk density, Archimedes method, inductive sensor, LC oscillator.

1. Introduction

Reliable density measurement is essential in laboratory research and serves as a starting point to analyse processes that occur in porous materials [1]. Depending on the cohesiveness of the sample, density measurement can be performed in various ways [2]. Inductive sensors are successfully used in our laboratory to measure the mechanical properties of rock samples (such as Poisson's ratio and Young's modulus) in a high-pressure chamber (up to 400 MPa), where they act as deformation sensors. It was decided to apply the advantages of the inductive sensor to density measurement as well [3]. The mathematical foundations of the resonance circuit operation in the Colpitts oscillator were formulated in [4]. The characteristics of the sensor, particularly its high sensitivity, prompted the development of a spring balance dedicated to accurate volume measurements of porous samples and determination of their bulk density.

Article history: received July 23, 2025; revised September 9, 2025; accepted November 17, 2025; available online November 24, 2025.

Bulk density, also referred to as envelope or geometric density, is one of the fundamental parameters used to describe the properties of porous materials. Rocks that are not continuous materials and, in addition to the solid phase, also contain voids of various shapes and sizes that make up their pore space [5]. The bulk density of a sample (most commonly denoted by ρ) is expressed as the ratio of mass to the total volume of the dried sample, including the pores contained within the sample. Knowledge of bulk density is essential to determine the void space in materials (open porosity). Bulk density and open porosity are crucial in assessing the durability of materials and, in studies of natural stone for construction purposes, they are determined as mandatory parameters [6].

In the case of regular-shaped samples, bulk density can be easily determined directly by dividing the mass of the sample by the volume calculated from its dimensions. For irregular samples, determining bulk density requires an accurate measurement of the sample's volume, which must account for all internal voids. Obtaining a precise value of the bulk volume of irregular and porous materials is not a simple task. It requires the use of methods such as mercury porosimetry, quasi-liquid (powder) pycnometry, or hydrostatic displacement [2, 7, 8]. Each of these methods has its advantages, but also certain limitations. Measurements of bulk density performed using mercury porosimetry or quasi-liquid pycnometry require expensive equipment. Additionally, porosimetry requires placing the tested sample in mercury, which is toxic and environmentally harmful [9]. In the quasi-liquid pycnometric method, strict control of measurement conditions is essential to obtain reliable results. The bed formed by the sample and powder must fill the measurement cell in appropriate proportions [2, 10]. The hydrostatic method, based on Archimedes' principle, offers a low-cost alternative to measure the bulk density of both regular and irregular samples [8, 11, 12]. Various structural designs of balances used in the Archimedes method, as well as different approaches to implementing the displacement method, are known [1, 13, 14]. This also applies to the sensors used for liquid level measurement, where among electrical, optical, and mechanical sensors, those based on optical technologies have been considered optimal [15].

This study presents a new version of the hydrostatic method for determining bulk density. The core of this method is the measurement of the volume of the tested sample using a custom-designed and built inductive spring balance. The novelty is that the springs are simultaneously the inductance sources of the LC oscillator resonance circuit. Changes in inductance caused by the change in the length of the spring under load cause a change in vibration frequency. The design of the spring balance is characterised by great simplicity and the transducer has a high sensitivity of 10^{-5}. The paper also presents the results of bulk density measurements of an aluminium block and porous sandstone using spring balance, which are compared with the results obtained using pycnometric methods.

2. Description of the spring balance

In bulk density measurements conducted using the innovative spring balance, an inductive weight-to-frequency transducer was used. In this transducer, the sensor consists of a pair of springs, which simultaneously serve as the inductance element of the LC oscillator's resonant circuit. Changes in the inductance, caused by the elongation of the springs under the load of the weighed object, lead to a changes in the oscillation frequency. Therefore, the measurement of weight essentially reduces to measuring the elongation of the springs. The schematic diagram of the spring balance, its general view, and an example sample prepared for suspension are shown in Fig. 1. The characteristics of the weight-to-frequency converter are shown in Fig. 2.

Metrol. Meas. Syst., Vol. 32 (2025), No. 4, pp. 1–14
DOI: 10.24425/mms.2025.155808

The construction of a spring balance with a weight-to-frequency transducer is quite simple. The only mechanically sensitive components of the balance are the sensors/springs, which are inexpensive and easy to obtain or manufacture independently. At this point, it is important to clarify the issue related to the use of the terms mass and weight. Balances measure weight, which is a force expressed in newtons (N). However, most balances are calibrated in units of mass, such as grams (g). As a result, there may be inconsistencies in terminology within the text, leading to phrases such as "a weight of 5 g", which is technically incorrect.

Fig. 1. Spring balance; a) schematic diagram, b) general view, c) sample prepared for suspension on a thin wire passing through an opening in the base of the balance.

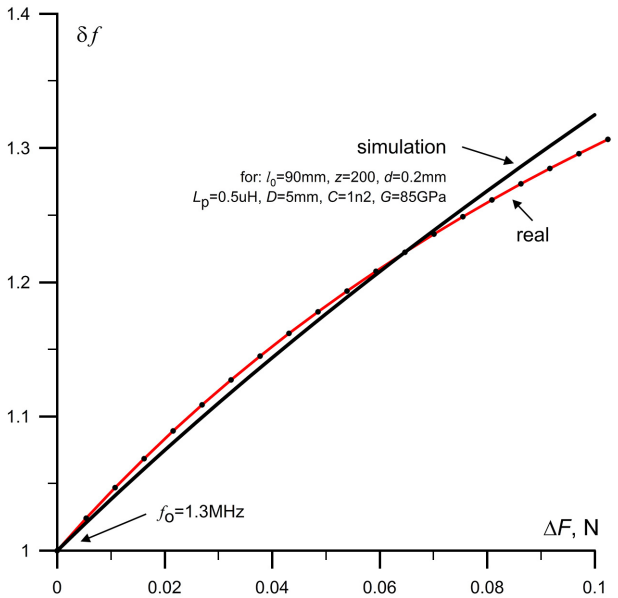

Fig. 2. Spring balance; comparison of relative frequency changes δf with the actual characteristic obtained by calibration.

The springs forming the sensor are connected electrically in series and mechanically in parallel. This design ensures that the electrical leads from the sensor to the oscillator are located on its fixed side. A thin wire is attached to the lower end of the sensor, passing outside the balance through an opening in the lower base of the housing. The weighed object is suspended from this rod (see Fig. 1c). The oscillator is best implemented using a Colpitts circuit [16, 17]. The short-term stability (minutes) of LC oscillators is approximately 10^{-6}, meaning that under ideal conditions (no mechanical vibrations or air movement), the presented balance can achieve a resolution of 10^{-6}. For example, a 10 g (full measurement range) can be measured with a resolution of about $3.0 \cdot 10^{-5}$ g. The accuracy of the measurement depends on both the calibration precision of the balance and the medium-term (hours) and long-term (days) stability of the oscillator. The main destabilising factors include temperature fluctuations around the oscillator and sensors and rheological phenomena in the springs during prolonged measurements (creep or relaxation effects). The oscillation frequency f of the resonant circuit is given by the following formula:

$$f = \frac{1}{2\pi\sqrt{(L_s + L_p) \cdot C}}, \quad L_s = \frac{\mu z^2 S}{l_s} \rightarrow f = \frac{\sqrt{1}_s}{2\pi\sqrt{\mu S C}} \text{ for } L_p = 0, \tag{1}$$

where L_s, L_p are inductances of the sensor itself and parasitic inductance (*i.e.*, connections to the oscillator), respectively, C is the total capacitance of the resonant circuit, l_s is the length of the sensor (in this case, the total length of the coils), μ, z, S are magnetic permeability, the number of turns of the coil/sensor, and the cross-sectional area of the coil/sensor, respectively (for an air-core coil, vacuum permeability can be assumed as $\mu = \mu_0$).

The connection between the sensor and the oscillator is very short (1 to 2 cm), so the value of parasitic inductances can be considered negligible. The elongation Δl_s of the loaded spring depends on its geometric dimensions and the material from which it is made, according to the following relationship:

$$\Delta l_s = \frac{F}{G}\frac{D^3}{d^4} = kF, \tag{2}$$

where F is the force acting on the spring (*i.e.*, the measured weight), G_s is the shear modulus (Kirchhoff's modulus) of the material from which the springs are made and D, d are the diameter of the spring and the diameter of the wire from which it is made, respectively. Then, the elongation of a single turn of the spring Δl_s^* is given by the formula:

$$\Delta l_s^* = 4\frac{F}{G}\frac{D^3}{d^4} \tag{3}$$

and the relative sensitivity of the spring s_l^*, defined as the ratio of the relative elongation of a single turn Δl_s^* to the incremental force ΔF that causes it, will be given by:

$$s_l^* = \frac{\Delta l_s^*}{\Delta F} = \frac{4}{G}\frac{D^3}{d^4}. \tag{4}$$

Equation (4) shows that to achieve high sensitivity of the spring as a weight sensor, the D/d ratio should be as large as possible.

Analysis of (1) and (4) shows that doubling the diameter of the coil D results in a fourfold increase in the cross-sectional area of the coil S, and consequently a fourfold increase in the inductance of the sensor L_s. At the same time, this is accompanied by a twofold increase in the length of the sensor l_s, which also doubles its resistance R. As a result, the relative sensitivity of the sensor can increase up to eight times, which is highly beneficial. However, excessive

increasing the coil diameter D while keeping the wire thickness constant leads to unstable coil positioning (variable distance and angle of inclination of the coils relative to each other), with a tendency for the coils to touch each other, causing short circuits and friction. In commercially manufactured springs, for wire diameters of less than 1 mm, the D/d ratio is typically limited to $10 \div 15$ to ensure sufficient spring reaction force to stretching. In the case of a spring balance, the appropriate reaction force is achieved by selecting the wire diameter. However, it is desirable to aim for a higher D/d ratio, ideally in the range of 17 to 20, which will result in high inductance and good electrical quality of the spring as a coil, sufficiently stable coil positioning, and most importantly, high sensitivity of the springs (sensors).

Increasing the spring length by increasing the number of coils, for example, four times, will also result in a fourfold increase in its inductance (see (1)). However, it will also lead to a fourfold increase in its resistance. As a result, the quality factor of the coil will decrease twofold. This is undesirable because for the quality factor of the resonant circuit to remain unchanged, it is necessary to reduce its capacitance by a factor of four. This, in turn, may cause the unstable parasitic capacitances to have a destabilising effect on the oscillations. In practice, the length of the unloaded spring is a few centimetres.

Taking into account (1) and (2), the weight-to-frequency transducer has a nonlinear characteristic, since the frequency change depends on the square root of the force:

$$f = \frac{1}{2\pi\sqrt{C}}\sqrt{\frac{l_o + \Delta l_s}{\mu z^2 S}} \text{ for } \mu = 4\pi 10^{-7}\frac{m \cdot T}{A} \text{ and } S = \frac{\pi D^2}{4} \rightarrow$$

$$f = \frac{1}{2\pi^2 D z\sqrt{C}}\sqrt{10^7\left(l_o + \frac{4zFD^3}{Gd^4}\right)} \approx \frac{160}{Dz\sqrt{C}}\sqrt{l_o + \frac{4zFD^3}{Gd^4}},$$

$$\text{but } l_o = \frac{160}{Dd^2}\sqrt{\frac{d^5G + 4DF}{zCG}}, \tag{5}$$

where l_o is the length of the unloaded (unstretched) spring. Fig. 2 shows the frequency-load dependence graph as a result of simulation using (5) and the actual curve obtained by calibration. The differences between the two curves originate from an imprecise estimation of the capacitance and inductance values of the parasitic connections between the sensor and the oscillator, as well as the value of the elasticity coefficient.

The sensitivity of the weight-to-frequency transducer s_f can be obtained by differentiating (5) with respect to force F applied to the balance. This gives:

$$s_f = \frac{\mathrm{d}f}{dF} \approx \frac{640D^2}{Gd^4\sqrt{C}\sqrt{l_o + \frac{4zFD^3}{Gd^4}}} \text{ for } L_p = 0. \tag{6}$$

A better parameter for characterising the sensor than absolute sensitivity is the relative sensitivity, defined as the ratio of the sensitivity from (6) to the oscillation frequency from (1), assuming negligible parasitic inductance ($L_p = 0$). This parameter describes the change in relative frequency under the influence of the applied force:

$$\frac{s_f}{f} = s_f^* \approx \frac{2}{\frac{d^5G}{D^3} + 4F}. \tag{7}$$

The relationships above are approximate, and, as in typical oscillators, the goal is to achieve the highest possible coil quality factor Q_L by minimising the distance between the turns, which is essential for ensuring maximum oscillation stability.

$$Q_L = \frac{X_L}{R_L} = \frac{2\pi f L}{R_L} = \frac{1}{R_L}\sqrt{\frac{L}{C}}, \tag{8}$$

where X_L and R_L are the reactance and resistance of the coil, respectively.

Estimating the value of this parasitic inductance is difficult. Therefore, the characteristic of the transducer should be determined by calibration. To obtain high accuracy in converting frequency changes to weight, the characteristic of the transducer should be approximated by a polynomial of at least the fourth degree.

Achieving a high quality factor of a coil used as a balance spring is difficult for two reasons: the coil is single-layered and lacks a magnetic core, and it has a high resistance because the spring steel used to make the spring has a high resistivity. Consequently, to achieve the required quality factor of the circuit, it is necessary to significantly reduce the capacitance of the resonant circuit (see (8)).

It should be emphasised that the parameters of the resonant circuit represent a compromise due to factors such as parasitic inductances and capacitances of the connections, capacitances of electronic components, spring sensitivity, and the quality factor of the resonant circuit. For example, in a prototype spring balance with a measurement range of up to 10 g, the sensor was made of spring steel wire with a resistance of $R = 30\ \Omega$, and the capacitance of the resonant circuit was $C = 1.3$ nF. The initial inductance of the 20 mm long spring (with coil spacing equal to wire diameter) was $L = 12\ \mu$H, and the oscillation frequency was $f = 1.3$ MHz, resulting in a resonant circuit quality factor of approximately 3.3. For the fully extended spring, the values were $L = 6\ \mu$H, $f = 1.75$ MHz, $Q = 2.2$. Despite such a low quality factor, the oscillations have a sufficiently high amplitude (0.3 V_{pp}) and stability, with fluctuations of only a few hertz.

3. Effect of temperature on measurement

Variations in the readings of the inductive spring balance due to temperature changes are the result of three factors: changes in resistance, and in the elasticity and thermal expansion coefficients of the spring material. First, an increase in temperature causes a decrease in the modulus of elasticity, so the spring will elongate with rising temperature under constant load. This will lead to a decrease in its inductance and consequently to an increase in oscillation frequency and an apparent increase in the measured weight. The modulus of elasticity decreases by approximately $10^{-3}/^{\circ}$C [18, 19], and the balance readings will increase by roughly this value. Second, a temperature rise increases the length of the spring wire (thermal expansion), resulting in a slight increase in the number of turns and consequently to an increase in inductance, which leads to a decrease in the oscillation frequency of the resonant circuit and an apparent decrease in the measured weight. Third, an increase in temperature causes an increase in resistance, leading to a drop in the oscillator's supply voltage, which also affects the oscillation frequency.

The impact of temperature on measurement can be reduced either through software – by applying mathematical corrections to the balance readings based on its thermal characteristics – or through hardware, by utilising the temperature dependence of coil resistance in a low-Q resonant circuit. In the presented balance, thermal compensation was achieved by exploiting the relationship between the oscillator's supply voltage and the oscillation frequency, incorporating a thermistor into the voltage stabiliser circuit. Fig. 3 shows the values of the thermal coefficient of relative

changes in the balance readings, δm, depending on the applied load. The oscillator parameters were selected so that the balance was thermally compensated within 80% of its maximum measuring range, as this is the range in which the balance is expected to be most frequently used.

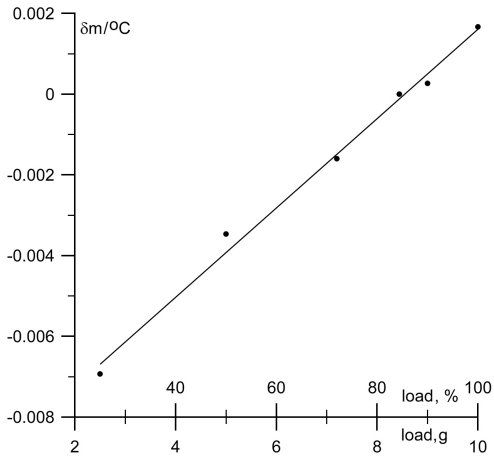

Fig. 3. Thermal coefficient of relative changes in balance readings vs. its load.

Figure 4 shows the relative measurement error of the weight due to changes in ambient temperature over a period of 5 days. The value of this thermal coefficient is approximately $10^{-4}/°\mathrm{C}$. Since the temperature influence is regular, this allows further reduction of its impact. The presented graph also indicates that the short-term stability of the balance readings, excluding the effect of temperature, is at a level of 10^{-5}. Minor disturbances appeared only between the 20$^{\text{th}}$ and 30$^{\text{th}}$ hour of recording.

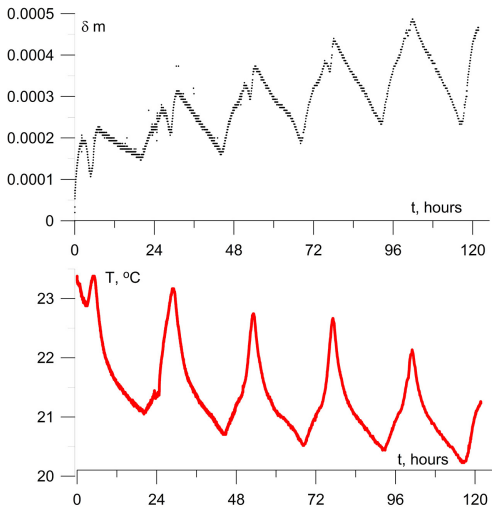

Fig. 4. Relative balance error (a) vs. ambient temperature (b).

4. Indication tests

4.1. Weight measurement

The spring balance was tested using standard weights of 10 g and 5 g ±2 mg. A series of 16 weight measurements was performed. Table 1 presents the average measurement results (from 16 trials) together with the relative measurement error. The deviation between the correct and actual values simulates errors in the procedure of measuring the weight of a sample soaked and taken from a liquid (in air) and a sample weighed in liquid, during density determination. The frequency changes were converted into weight values using polynomial approximations of the characteristic curve (see Fig. 2) with polynomials of the second, fourth and sixth degree.

Table 1. Measurement test for calibration weights of 10 g and 5 g.

Polynomial degree	**2nd**	**4th**	**6th**	**Standard deviation**
Δm (10 g–5 g), mean	5.04495 g	5.00312 g	5.00179 g	
δm (10 g–5 g)/5 g, mean	$9.0 \cdot 10^{-3}$	$2.6 \cdot 10^{-3}$	$0.36 \cdot 10^{-3}$	$0.15 \cdot 10^{-3}$
5g, mean	4.93749 g	4.94723 g	4.94742 g	
δm (5 g), mean	$-12 \cdot 10^{-3}$	$-11 \cdot 10^{-3}$	$-10 \cdot 10^{-3}$	$0.0021 \cdot 10^{-3}$
10 g, mean	9.98244 g	9.95035 g	9.94920 g	
δm (10 g), mean	$-1.7 \cdot 10^{-3}$	$-5.0 \cdot 10^{-3}$	$-5.1 \cdot 10^{-3}$	$0.10 \cdot 10^{-3}$

Analysing the values recorded in Table 1, it can be concluded that the measured weight for both 5 g and 10 g was lower than the actual values, probably due to inaccurate determination of the spring balance characteristic curve. Despite this, the calculated weight difference between these weights was small, with a relative error of δm ((10 g–5 g)/5 g) = $0.36 \cdot 10^{-3}$, for the polynomial approximation of the sixth degree. The second-degree polynomial approximation is not recommended (relative error of $\delta m = 9 \cdot 10^{-3}$). The calibration measurement for the 5 g weight was performed with a very small standard deviation of $0.0021 \cdot 10^{-3}$, due to effective suppression of mechanical oscillations in the springs. For the 10 g measurement, the mechanical oscillations were more pronounced, leading to a greater measurement spread.

4.2. Density measurement

The procedure for determining the bulk density of rocks using the hydrostatic displacement method is recommended both by the standards currently in force in the European Union [20,21] and by the International Society for Rock Mechanics [22]. It is also a standard testing method for highly porous light materials [23]. In the case of a rock that absorbs the displacement liquid, the sample should first be weighed in a dry state and then saturated with the liquid. After saturation, the sample should be weighed in air and in liquid. In this case, the bulk density ρ is given by the formula:

$$\rho = \rho_{rh} \frac{m_d}{m_{sa} - m_{sh}}, \tag{9}$$

where m_{sa} and m_{sh} are the masses of the saturated sample measured in air and in liquid, respectively. For samples that do not absorb the liquid, $m_{sa} = m_d$.

Test density measurements were conducted on objects with regular geometry to allow for the calculation of their density by determining the volume of the sample through dimensional measurements using a micrometer screw gauge and weighing them with a laboratory balance. This method of calculating volume using a micrometer is referred to as the geometric method. The volume of the sample was also measured using professional pycnometers: the helium method for accurately determining skeletal density (ρ_s), and the quasi-liquid method for measuring bulk density ρ, using the AccuPyc 1340 and GeoPyc 1360 (Micromeritics Instrument Corporation, Norcross, GA, United States), respectively. In the displacement method, a water density of 0.998 g/cm^3 was assumed. The samples tested included a ground aluminium cuboid with dimensions of 17.5 mm × 18.0 mm × 10.0 mm and a mass of 8 g, as well as porous Tumlin sandstone (Fig. 5).

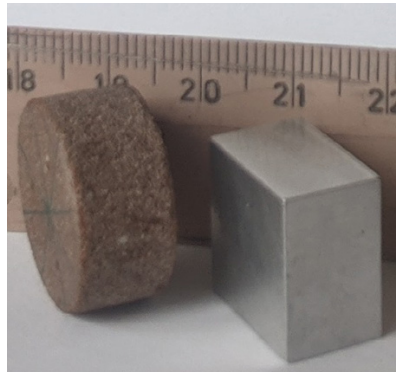

Fig. 5. Samples for density measurements using the spring balance: sandstone cylinder on the left and aluminium cuboid on the right.

4.2.1. Measurement of volume and density of the aluminium block

In the case of aluminium, which is a non-porous material, its bulk density is equal to its true (skeletal) density ($\rho = \rho_s$), and the bulk volume and bulk density of the aluminium sample could be measured using all four methods. Table 2 presents the results of these measurements, with several repetitions performed for each method.

Table 2. Testing density and volume with different measurement methods: aluminium.

Aluminium	V, cm^3	ρ, g/cm^3	**Number of Measurements**	**Standard Deviation** σ	$\delta\rho$: **x/He**
Helium Pycnometry	3.1460	2.798	16	$0.27 \cdot 10^{-3}$	0
Spring Balance Method	3.128	2.801	16	$0.19 \cdot 10^{-3}$	$1.1 \cdot 10^{-3}$
Powder Pycnometry	3.1473	2.964	10	$4.2 \cdot 10^{-3}$	$59 \cdot 10^{-3}$
Micrometer screw gauge	3.1627	2.783	10	$7.3 \cdot 10^{-3}$	$-5.3 \cdot 10^{-3}$

The measurement results presented in Table 2 allow for the following conclusions:

1. The measurement variability – expressed as the standard deviation (fifth column) – is the smallest for measurements performed using the spring balance.
2. The spring balance method shows the lowest value of the difference $\delta\rho$ compared to the helium method, which is considered the most accurate.

3. The highest $\delta\rho$ value – almost 6% – was observed with the powder method.
4. The greatest variability in measurement results occurred when the volume was determined using a micrometer, which is a consequence of inaccuracies in grinding of the aluminium cuboid.

4.2.2. Measurement of volume and density of sandstone

Tumlin sandstone, with a porosity of approximately 7.5%, was selected for the study as a representative porous material that absorbs water. It was characterized by a high structural uniformity, which is essential for measurements of samples with different dimensions. For such a material $\rho \neq \rho_s$, and the helium method cannot be used to determine its bulk volume. Therefore, the results of bulk density determination using the spring balance were compared only with those obtained using the powder method and the geometric method, where volume was determined using a micrometer. Three cylindrical samples of different sizes were prepared to estimate the influence of sample size on measurement results. Table 3 presents the averaged results from 16 measurements. The first column provides the sample diameter d and height h, the second shows the weight measurement results obtained using the laboratory or spring balance. The third column contains the calculated density of the samples based on volume measured with a calliper or the powder method, and the weight measured with either the laboratory or spring balance. The last column presents the standard deviation value of the density calculation across the 16 measurements.

The largest sample ($d = 32$, $h = 80$) was too heavy for density measurement using the spring balance and too large for the powder method. It was assumed that the weight measurement using a laboratory balance is sufficiently accurate, so any errors in the calculated density are solely attributed to volume measurement errors – whether using the geometric or powder method.

Table 3. Results for testing density with different measurement methods: Tumlin sandstone.

Sample, mm	**Dry Mass, g**	**ρ, g/cm^3**	**$\sigma\rho$, per mille**
$d = 32$, $h = 80$	Laboratory Balance: 119.42	Calliper: 2.422	0.71
$d = 22$, $h = 45$	Laboratory Balance: 43.885	Calliper: 2.389, Powder: 2.4501	1.8 2.9
$d = 22$, $h = 9$	Laboratory Balance: 9.037	Calliper: 2.390 Powder: 2.3932	3.1 13
$d = 22$, $h = 9$	Spring Balance: 9.045	Spring Balance: 2.432	1.5

The apparent density values summarised in Table 3 are presented graphically in Fig. 6.

The most reliable density measurement probably refers to the largest sandstone sample as, in this case, the relative error from surface grinding and dimensional measurements is the smallest. This assumption is supported by the lowest measurement variability in this case ($\sigma = 0.071\%$). If this assumption is considered justified and this density is taken as the reference value, then the results presented in Table 3 allow for the formulation of the following conclusions:

1. The most accurate density measurement was obtained using the spring balance, which was used to measure both the weight and the volume of the sandstone. The calculated density was only 0.4% higher compared to the reference value.
2. The density measured using both the powder and geometric methods for the small and medium samples was approximately 1.7% lower compared to the reference value. This is most probably caused by the granular structure of sandstone. In such cases, the sample's bases and lateral surface cannot be perfectly flat, and the calliper measures "over the peaks

of irregularities," resulting in overestimated volume measurements. This also applies to the powder method, due to the incomplete surrounding of the sample by the powder in the instrument's container, which leads to an overestimated measured volume.

3. An exception is the density measurement using the powder method for the medium sample (h = 45 mm, d = 25 mm), which yielded a value 1.1% higher than the reference sample. The cause of this deviation from the other measurements may be the use of a different, larger powder container.
4. The measurement variability for the small sample using the powder method is $\sigma = 1.3\%$, which corresponds to the repeatability declared by the manufacturer in the GeoPyc 1360 device manual V3.01/2001, stated as $+/-1\%$. The measurement variability using the spring balance is $\sigma = 0,15\%$, which must be considered a significantly better result. It should be emphasized that the specifications provided by the manufacturer of the GeoPyc 1360 device do not include information on the accuracy of the performed measurements (see GeoPyc 1360 Envelope Density Analyzer, *n.d.*).

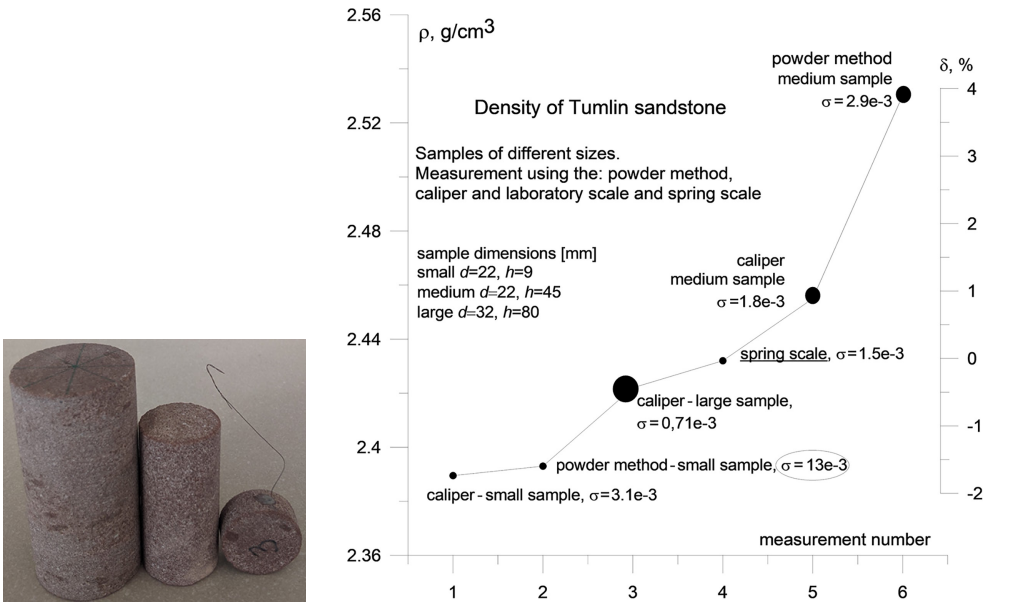

(a) (b)

Fig. 6. Results of the Tumlin sandstone density measurements for samples of different sizes (a) using various methods, along with the deviation of the measurements relative to the density measured with a spring balance (b).

5. Uncertainty of bulk density measurement using the spring balance

The uncertainty of bulk density measurement involves determining the density of the liquid and weighing the sample in its dry state (in air), in its saturated state (in air, for samples that absorb the displacement liquid), and in its saturated state when submerged in the displacement liquid.

The estimated balance of relative uncertainties is as follows:

– uncertainty of water density: $u_w = 0.2 \cdot 10^{-3}$,
– threefold uncertainty in determining the characteristics of the balance (three weighings of the sample, geometric sum): $u_c = 1.5 \cdot 10^{-3}$,

– twofold uncertainty related to mechanical vibrations of the springs during the weighing of the dry and saturated sample removed from the liquid: $u_d = 0.5 \cdot 10^{-3}$,
– uncertainty of the procedure for removing excess liquid from the sample: $u_s = 1.0 \cdot 10^{-3}$,
– uncertainty related to liquid evaporation: $u_p = 0.5 \cdot 10^{-3}$,
– uncertainty caused by air bubbles attached during weighing of the sample in the liquid: $u_b = 0.5 \cdot 10^{-3}$.

By summing all the above uncertainty components geometrically, the final formula for the uncertainty of the bulk density measurement obtained is as follows:

$$\begin{aligned} u_\rho &= \sqrt{u_w^2 + 3(u_c)^2 + 2\,(u_d)^2 + u_s^2 + u_p^2 + u_b^2} \\ &= 10^{-3}\sqrt{0.2^2 + 3 \cdot 0.5^2 + 2 \cdot 0.5^2 + 1 + 0.5^2 + 0.5^2} = 1.67 \cdot 10^{-3}. \end{aligned} \tag{10}$$

Thus, the calculated total relative uncertainty of the bulk density measurement is $u_\rho = 1.67 \cdot 10^{-3}$. Assuming an expanded uncertainty coefficient $k = 1.65$ for a rectangular distribution (finite range), we obtain a final uncertainty value of $u_\rho = 2.8 \cdot 10^{-3}$, corresponding to a confidence interval of approximately 95%. This value aligns well with the uncertainty calculated from the test measurement results presented below.

6. Final Conclusions

The use of a spring balance to determine volume and bulk density via the hydrostatic displacement method in liquid is fully justified. This applies to both absorbent and non-absorbent materials with respect to the measuring liquid. The uncertainty of bulk density measurement using the spring balance for non-absorbent samples can be estimated at a few per mille. For absorbent samples, this uncertainty is higher, around 1%, due to uncertainties related to saturation, removal of excess liquid from the sample during weighing in air, and evaporation of the liquid during weighing.

The powder method involves several times greater uncertainty in bulk density measurement compared to the liquid method, as demonstrated by the test results presented in this article. The powder method is less labour-intensive because it does not require saturation, wiping, or multiple weighings of the sample. The "classical" method, which involves determining the sample volume based on its geometry, is only applicable to regular-shaped samples. Obtaining sufficient geometric regularity in rock samples is difficult and, in most cases, impossible. The design of the spring balance with a weight-to-frequency converter is inexpensive and mechanically simple as well as in terms of its electronic circuitry. The metrological parameters of the inductive spring balance presented in this article allow its use in real-time recording and visualisation of the dynamics of liquid or moisture absorption by a sample. The results of such studies will be the subject of a subsequent publication.

Acknowledgements

This work was supported by the Ministry of Science and Higher Education in Poland. The funding involved a project entitled: Station for measuring bulk density and moisture sorption using a high-sensitivity spring balance [grant number FBW/D/2023–2024/02/2024], financed from the Scientific Research Fund of the Strata Mechanics Research Institute of the Polish Academy of Sciences.

References

[1] Park, S., Kang, M., Oinam, Y., Amoozegar, A., & Pyo, S. (2022). Measurement of skeletal density and porosity of construction materials using a new proposed vacuum pycnometer. *Measurement*, *196*, 111209. https://doi.org/10.1016/j.measurement.2022.111209

[2] Zhao, C., Zhou, W., Hu, Q., Xu, H., & Zhang, C. (2021). Porosity measurement of granular rock samples by modified bulk density analyses with particle envelopment. *Marine and Petroleum Geology*, *133*, 105273. https://doi.org/10.1016/j.marpetgeo.2021.105273

[3] Nurkowski, J., & Nowakowski, A. (2023). Inductive sensor for measuring linear displacement and velocity – Version with stationary magnetic core. *Measurement*, *222*, 113675. https://doi.org/10.1016/j.measurement.2023.113675

[4] Nurkowski, J., & Nowakowski, A. (2022). Thermally compensated inductive deformation sensor – Mathematical background and practical implementation. *Measurement*, *197*, 111282. https://doi.org/10.1016/j.measurement.2022.111282

[5] Nowakowski, A., & Nurkowski, J. (2023). About some problems related to determination of the *e.g.* the Biot coefficient for rocks. *Archives of Mining Sciences*. https://doi.org/10.24425/ams.2021.136697

[6] Strzałkowski, P. (2018). Requirements and Test Methods for Selected Natural Stone Products (in Polish). *Górnictwo Odkrywkowe*, *59*, 34–40.

[7] Serway, R., Jewett, J. (2008). *Physics for Scientists and Engineers with Modern Physics*. Seventh Edition. Thomson Higher Education.

[8] Agrawal, S. (2021). Simplified Measurement of Density of Irregular Shaped Composites Material Using Archimedes Principle by Mixing Two Fluids Having Different Densities. *International Research Journal of Engineering and Technology*, *8*, 1005–1009. https://doi.org/10.1107/S002188986800542X

[9] Washburn, E. W. (1921). Note on a method of determining the distribution of pore sizes in a porous material. *Proceedings of the National Academy of Sciences*, *7*(4), 115–116. https://doi.org/10.1073/pnas.7.4.115

[10] Godyń, K., & Dutka, B. (2021). Sorption and Micro-Scale strength properties of coals susceptible to outburst caused by changes in degree of coalification. *Materials*, *14*(19), 5807. https://doi.org/10.3390/ma14195807

[11] Ledwaba, T., Mbuyisa, B., Blakey-Milner, B., Steenkamp, C., & Du Plessis, A. (2023). X-ray computed tomography vs Archimedes method: a head-to-head comparison. *MATEC Web of Conferences*, *388*, 08002. https://doi.org/10.1051/matecconf/202338808002

[12] Mohazzab, P. (2017). Archimedes' principle revisited. *Journal of Applied Mathematics and Physics*, *05*(04), 836–843. https://doi.org/10.4236/jamp.2017.54073

[13] Bruce, D., Paradise, P., Saxena, A., Temes, S., Clark, R., Noe, C., Benedict, M., Broderick, T., & Bhate, D. (2022). A critical assessment of the Archimedes density method for thin-wall specimens in laser powder bed fusion: Measurement capability, process sensitivity and property correlation. *Journal of Manufacturing Processes*, *79*, 185–192. https://doi.org/10.1016/j.jmapro.2022.04.059

[14] Sizov, A., Mihiretie, B., Ma, Y., Gustafsson, S. E., & Gustavsson, M. (2023). Thermal conductivity vs depth profiling using the hot disk technique — Analysis of anisotropic, inhomogeneous structures. *Review of Scientific Instruments*, *94*(7). https://doi.org/10.1063/5.0145902

[15] Ramos, C. C., Preizal, J., Hu, X., Caucheteur, C., Woyessa, G., Bang, O., Rocha, A. M., & Oliveira, R. (2025). High resolution liquid level sensor based on Archimedes' law of buoyancy using polymer optical fiber Bragg gratings. *Measurement*, *252*, 117368. https://doi.org/10.1016/j.measurement.2025.117368

[16] Horowitz, P., Hill, W. (2015). Oscillators and Timers. *The Art of Electronics*, 425–470. Cambridge University Press.

[17] Pawłowski, J. (1980). Wzmacniacze i generatory (*Amplifiers and Generators*). Wydawnictwa Komunikacji i Łączności. Warszawa.

[18] Kou, H., Gao, Y., Shao, J., Dou, K., & Wang, N. (2022). Temperature-porosity-dependent elastic modulus model for metallic materials. *Reviews on Advanced Materials Science*, *61*(1), 769–777. https://doi.org/10.1515/rams-2022-0270

[19] Li, W., Kou, H., Zhang, X., Ma, J., Li, Y., Geng, P., Wu, X., Chen, L., & Fang, D. (2019). Temperature-dependent elastic modulus model for metallic bulk materials. *Mechanics of Materials*, *139*, 103194. https://doi.org/10.1016/j.mechmat.2019.103194

[20] European Committee for Standardization. (2008). *Natural Stone Test Methods Determination of Real Density and Apparent Density, and of Total and Open Porosity*. EN-1936.

[21] International Organization for Standardization. (2018). *Ceramic Tiles. Part 3: Determination of Water Absorption, Apparent Porosity, Apparent Relative Density and Bulk Density*. EN ISO 10545-3.

[22] Franklin, J.A., Vogler, U.V., Szlavin, J., Edmond, J.M. & Bieniawski, Z.T. (2007). *Suggested Methods for Determining Water Content, Porosity, Density, Absorption and Related Properties and Swelling and Slake-Durability* (pp. 143–151). [Ulusay, R., Hudson, J.A. (Eds.) The Complete ISRM Suggested Methods for Rock Characterisation, Testing and Monitoring 1974–2006, ISRM Turkish National Group, Ankara]

[23] Moradi, A., Pramanik, S., Ataollahi, F., Kamarul, T., & Pingguan-Murphy, B. (2014). Archimedes revisited: computer assisted micro-volumetric modification of the liquid displacement method for porosity measurement of highly porous light materials. *Analytical Methods*, *6*(12), 4396–4401. https://doi.org/10.1039/c4ay00666f

Janusz Nurkowski has been an employee of the Polish Academy of Sciences (PAN) since 1988. In 2021, he obtained his PhD in technical sciences from the PAN. His research focuses on the measurement of rock deformation under normal conditions and high hydrostatic pressure. He is the author and co-author of measuring devices based on displacement-frequency transducers, as well as several articles published in scientific journals and conference proceedings. Most recently, he has been working on the application of such transducers in the construction of precision scales.

Barbara Dutka is an assistant professor at the Strata Mechanics Research Institute of the Polish Academy of Sciences in Kraków. In 2017, she obtained her Ph.D. in technical sciences in the field of mining and engineering geology. She specialises in sorption processes and analysis of the porous structure of materials. She is committed to working in the field of waste management, particularly in the search for possible use of municipal solid waste incineration bottom ash. She is the author of over 50 journal and conference publications. She is the coordinator of the Polish–Romanian research project for 2023–2026 named "Macro and micro strength tests on composite–cement stones".

Maciej Tram is a researcher at the Strata Mechanics Research Institute of the Polish Academy of Sciences in Kraków, where he develops solutions for municipal solid-waste utilisation, bottom-ash valorisation, and circular-economy applications. He is pursuing a PhD from Cracow University of Technology, working on optical thin-film coatings and their characterisation through spectrophotometry and ellipsometry. He has authored and co-authored several publications and has contributed to national and international research projects in materials engineering, environmental technologies, and advanced characterisation methods.